



# Effects of Nitrogen Atoms in Vindoline Alkaloids as $\text{Fe}^{2+}$ Ions Inhibitor in Corrosion of Gray Iron in Dilute HCl Environment: Potentiodynamic Polarization, Gravimetric Analysis and SEM

B. U. Ugi

Department of Pure & Applied Chemistry, University of Calabar, P. M. B. 1115, Calabar – Nigeria.

Received 19 June 2020,  
Revised 13 July 2020,  
Accepted 15 July 2020

**Keywords**  
✓ Vindoline,  
✓ alkaloids,  
✓ SEM,  
✓ Adsorption,  
✓ polarization.

[ugibenedict@gmail.com](mailto:ugibenedict@gmail.com)  
Phone: +234-7067921098

## Abstract

Effects of Nitrogen Molecule ( $\text{N}_2$ ) in Vindoline Alkaloids as  $\text{Fe}^{2+}$  Ions Inhibitor in Corrosion of Mild Steel in Dilute HCl Environment was investigated through the aid of both Potentiodynamic polarization method, Gravimetric and Scanning electron microscopic (SEM) methods. Results from this research showed strong molecular collision and adsorption of Vindoline particles on the Gray Iron in 1 M Hydrochloric Acid Solutions as inhibition efficiency from both electrochemical and chemical (gravimetric) measurements stood at 94.2 and 99.0 % respectively. Both corrosion rates and corrosion current densities of Gray Iron in 1 M Hydrochloric Acid Solutions were found to be decreasing with increased concentration of inhibitor. From the thermodynamic data, the inhibitors had the potential of influencing the incoming energy in the system resulting in higher potential energy and lower kinetic energy. Vindoline inhibitor presented a mixed type inhibition responsible for both reduction in anodic dissolution and cathodic hydrogen gas evolution. The inhibitor was stabled, spontaneous in the forward direction, physically adsorbed, associative and endothermic in nature. It obeyed both Langmuir and Temkin adsorption isotherms hence a monolayer adsorption and a characteristic uniform distribution of binding energies at various temperatures.

## 1. Introduction

The presence of iron in everyday life has a very long history way back to the 1200 BCE, encompassing a wide range of uses from farming implements to weapons of war. Blacksmiths became a critical profession, working with iron to change its properties and shape the material into tools such as sickles, plowshares, nails, swords, candlestick holders, etc [1]. The discovery of iron's value led to what has become known as the Iron Age, due to the dominance of this material in social and military applications. Corrosion is the gradual deterioration of materials, usually metals, or their properties by chemical reactions with the environment [1,2]. However, due to the increased use of metals in the modern world, corrosion can cause enormous loss if it occur. A steel surface contains both cathodic and anodic sites. In the presence of a layer of conducting solution, water electrons are more likely to pass from anodes to cathodes. Thus anode deficiency in electrons leads to oxidation and subsequently corrosion. There are several ways to accomplish corrosion protection and all these ways depend mainly but limited to environmentally friendly disposition of the protection measure [1-3]. This factor gave rise to the adoption of corrosion inhibitor by researchers in the struggle to find a lasting solution to corrosion

effects. Corrosion inhibitors function by forming a protective film on the metal surface. The functionality of these inhibitors depends on the change of anodic or cathodic polarization behavior and the decrease in the diffusion of ions to the surface of the metal [1-2].

Gray iron is characterized by the flake shape of the graphite molecules in the metal. When the metal is fractured, the break occurs along the graphite flakes, which gives it the gray colour on the fractured metal's surface. Gray iron is easier to machine and its wear resistance properties make it one of the highest volume cast iron products. Gray iron has the following composition: Carbon (2.5 %), Silicon (1.0%), Manganese (0.2 %), Sulphur (0.02 %), Phosphorus (0.02 %) and the rest Iron. Gray iron is used to make engine blocks and cylinder heads, manifolds, gas burners, gear blanks, enclosures, housing, etc [1]. Vindoline ( $C_{25}H_{32}N_2O_6$ ) is an indole alkaloid that exhibits antimetabolic activity by inhibiting microtubule assembly (Figure 1). It is a vinca alkaloid, an alkaloid ester, an organic heteropentacyclic compound and a methyl ester. It is a conjugate base of a vindolinium (1+) [4].

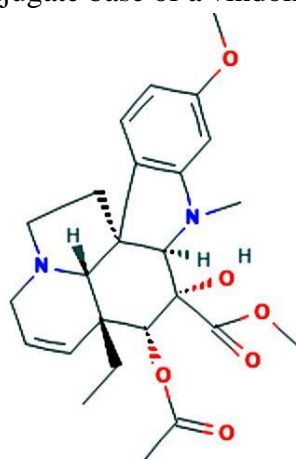


**Figure 1:** Structure of Vindoline alkaloid

As earlier mentioned, the dependency of the corrosion protection measures on the environmentally friendly nature of inhibitor lead to the researcher's interest in this area of research and also the novelty nature of the research sample and site. This research is aimed at investigating Vindoline particles of Vinca Alkaloids from *Cetharanthus roseus* Plant as electrochemical corrosion control inhibitor for Gray Iron in 1 M Hydrochloric Acid Solutions.

## 2. Material and Methods

### 2.1 Preparation, extraction and isolation of Vindoline alkaloid

The leaves of *Cetharanthus roseus* plant that were collected from a local bush in Becheve community in Cross River State, Nigeria and identified at the Botany Department University of Calabar were washed with mild water and air dried for 24 hours before oven dried for 48 hours at 55°C. The dried leaves were later grounded to nano-size and sieved. One hundred and fifty grams of the powdered material was extracted with 250 ml ethanol in a Soxhlet extractor with the heat supplied by a heating mantle at controlled temperature. The mixture of crude extract and ethanol was evaporated through the aid of a water bath at 60°C. The crude extract was used to isolate the vindoline alkaloid.

50 g of the evaporated extract was acidified with 5 ml of 2% tartaric acid. 100 ml of diethylether was used to digest the acidified extract to enable the extraction of chlorophyll, neutral alkaloids and other neutral compounds. The diethylether was later filtered off. The tartaric acid layer was removed and adjusted to a pH of 5.9 with ammonium hydroxide solution. The neutral alkaloids were collected in the organic phase after basification. The two separated liquids were further extracted to obtain individual

alkaloid rich extracts. The remaining diethylether layer was washed three times with distilled water and water decanted and organic layer dried over anhydrous sodium sulphate. The dried organic layer was dissolved in 5 ml methanol and 1 g activated charcoal and stirred for 10 min. and the solution filtered. The solution was later evaporated in a water bath and shaken for 1.30 min. On cooling, vindoline formed crystals and separated at the bottom of the flask. The crystals were then filtered and the slurry charged to the drier to obtain dry powder according to Chandrasekaran et al. [4].

### 2.2 Preparation of vindoline alkaloid inhibitor

10 g of the vindoline alkaloid extract was weighed into a 1000 ml volumetric flask and 1 M HCl solution was introduced. The content was well shook and allowed for 24 hours to complete digestion. The content was later filtered and serial dilution of the now inhibitor was prepared at  $2.2 \times 10^{-3}$ ,  $4.4 \times 10^{-3}$ ,  $6.6 \times 10^{-3}$ ,  $8.8 \times 10^{-3}$  and  $1.1 \times 10^{-2}$  MolL<sup>-1</sup>.

### 2.3 Weight loss experimentation

The weight loss measurements was conducted under an ambient temperature with the aid of polished resized Gray Iron coupons (3.5 x 3.5 x 0.5 cm<sup>2</sup> dimension) already prepared and washed, degreased, rinsed and air dried, then stored in an air free desiccator. The various concentrations of the vindoline alkaloid inhibitors were measured and decanted into different 100 ml graduated beakers including the raw diluted acid. The prepared metals were introduced into the solutions after initial measurements of their weight were taken and recorded. After 3 hrs of immersion, the metals were removed and washed in distilled water, degreased with ethanol, rinsed with acetone and air dried then weighed and recorded. This process continued for another 15 hours and triplicate results were obtained and averaged.

### 2.4 Potentiodynamic polarization experiment

Potentiodynamic polarization experiment for the corrosion of Gray Iron in 1 M Hydrochloric Acid Solutions was performed in both 1M HCl solution with and without serial concentrations of VACR (1.0 and 5.0 g/L) using Princeton Applied Research Model 263A Potentiostat/Galvanostat. A three electrode test flask was use with the Gray Iron resized metal (1 x 1 cm dimension) as the working electrode, platinum wire as the counter electrode and the saturated calomel electrode as the reference electrode. The experiment commenced immediately after the Gray Iron sheet was allowed to corrode freely and its open circuit potential was obtained as a function of time for 1800 sec. The tafel plots were obtained by altering the electrode potential from - 0.15 to + 0.15 V with respect to OCP at a scan rate of 0.2 mV/s. The data for corrosion density ( $I_{\text{corr}}$ ) and corrosion potential ( $E_{\text{corr}}$ ) were acquired automatically using Versa Studio software. The inhibition efficiency was calculated from equation 1.

$$E.I\% = 100 \left[ 1 - \frac{I_{\text{corr}}^{\text{p}}}{I_{\text{corr}}^{\text{i}}} \right] \quad 1$$

where  $I_{\text{bcorr}}$  and  $I_{\text{corr}}$  is the corrosion density in the absence and presence of VACR respectively.

### 2.5 Scanning electron microscopy

Phenom Pro Scanning electron microscope was used (Figure 2) in the examination of the relationship between the inhibitor adsorption and the metal surface reactivity. The Phenom Pro is Phenom-World's high-end imaging desktop SEM. In combination with a large range of sample-holders and automated system software, it can be tailored to suit a multitude of applications. 10 kV acceleration voltage was maintained for outstanding high-resolution SEM images.



**Figure 2:** Phenom Pro Scanning electron microscope

### 3. Results and discussion

#### 3.1 Weight loss measurements

The weight loss or mass loss experimentation allows one to determine to the nearest certainty the amount of material loss from a metal with respect to the effect of both temperature and acid attack. From [Table 1](#), it was observed that the mass of material loss from the metal as it came in direct contact with the 1 M HCl acid solutions without the vindoline alkaloid fraction was much higher compared to the loss as various concentrations of the vindoline alkaloid fractions were varied positively. This was explained on the basis that the exposed surface area of the metal, most importantly that which hosted the anodic sites prone to losing of electron giving rise to oxidation (corrosion), was interfaced by the nitrogen atoms in the vindoline alkaloids such that increasing the concentration of the alkaloids, decreased the direct acid contact with the surface, hence inhibiting the metal [\[5-8\]](#). The inhibition efficiency was also found to be 99.0 % at the highest experimental concentration of 5.0 g/L indicating that a further increase in the inhibitor concentration may not have any further inhibiting effect on the surface, hence the inhibitor at that concentration was able to replace almost all the water molecules on the metal surface and again reduce the frequent transfer of ions from the anodic sites which would have given room for a subsequent corrosion reaction [\[6, 9-12\]](#). It is gathered from this results that the vindoline particles of *Vinca Alkaloids of Cetharanthus roseus* plant are very good inhibitors for the electrochemical corrosion control of Gray Iron in 1 M Hydrochloric acid solutions.

**Table 1.** Representation of the corrosion rate of Gray Iron, surface coverage and inhibition efficiency of vindoline particles of *Vinca Alkaloids of Cetharanthus roseus* plant in 1 M HCl solutions at ambient temperature. M = 456.5 g/mol

Conc. (mol/L)	CR (mg/cm <sup>2</sup> /h)	$\theta$	%IE
1 M HCl	0.910	-	-
$2.2 \times 10^{-3}$	0.300	0.670	67.0
$4.4 \times 10^{-3}$	0.219	0.759	75.9
$6.6 \times 10^{-3}$	0.152	0.833	83.3
$8.8 \times 10^{-3}$	0.087	0.904	90.4
$1.1 \times 10^{-2}$	0.009	0.990	99.0

#### 2.2 Potentiodynamic polarization analysis

From the Potentiodynamic polarization curves in [Figure 3](#), the following data from the curve,  $E_{\text{corr}}$ ,  $i_{\text{corr}}$ ,  $ba$  and  $bc$  as seen in [Table 2](#) were obtained in order to analyze the result. Result of corrosion current density showed an appreciable decrease in the presence of the vindoline alkaloid compared to that

without the inhibitor. This was confirmed from the result of inhibition efficiency of 94.2 % and surface coverage. The striking point here is the agreement of the Potentiodynamic result with that of the weight loss claiming the reliable status of the inhibitor. However, the nature of the electrochemical result explained the strong molecular binding of the inhibitor to the tried surface at increasing concentration according [7-8, 13-16]. This can also be due to the fact that the corrosion rate of Gray Iron in 1 M Hydrochloric acid solutions is almost always rate limited by the cathodic reaction and by the mass transport of oxidizers (dissolved oxygen) to the surface hence, giving way for more inhibition at the anodic dissolution site of the metal [17-21]. From Table 2 also, the corrosion potential values were seen to be less negative as inhibitor concentration is increased, signifying that the system will rather take up electrons than loose electrons, so a reduction is more likely than oxidation of the metal and the inhibitor is a mixed type inhibitor but with preference to the anodic inhibition [12, 15, 20-25].

**Table 2:** Representative data from PDP showing effects of inhibition of vindoline particles on Gray Iron in 1 M HCl solutions.

Conc. (mol/L)	$I_{corr}$ (mAcm <sup>-2</sup> )	$-E_{corr}$ (mV)	bc (mV/dec)	ba (mV/dec)	$\theta$	IEi (%)
1 M HCl	11.857	293	119	127	-	-
$2.2 \times 10^{-3}$	3.283	182	83	94	0.723	72.3
$1.1 \times 10^{-2}$	0.684	104	56	17	0.942	94.2

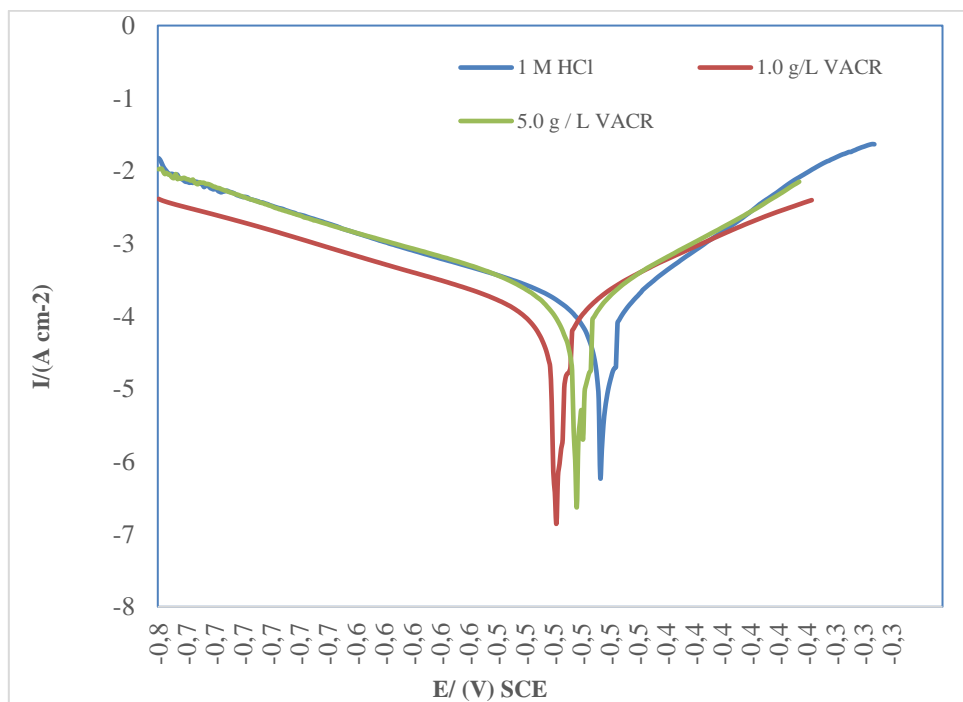


**Figure 3:** Tafel plots for the inhibition of vindoline particles on Gray Iron in 1 M HCl solutions.

### 2.3 Morphological examination

SEM was used to analyze the surface morphology in detail to identify surface changes or defects [19,28]. The ability to understand surface morphology allows results to be obtained in a rapid and easy manner. The surface of the metal in the absence of the vindoline inhibitor (i.e. pure 1 M HCl) as presented in Figure 4a showed so much cracks, tie and wear. An indication that the free acid had a reasonable surface

occupancy, hence attacking the metal surface rudely [19-21]. Figure 4b showed less attacked by the acid as inhibitor addition reduced the corrosion interaction reaction with the surface and subsequent increase in concentration up to 5 g/L led to blocking of the active sites on the metal that could allow corrosion reaction process, hence inhibiting strongly the acid corrosion [29, 33].

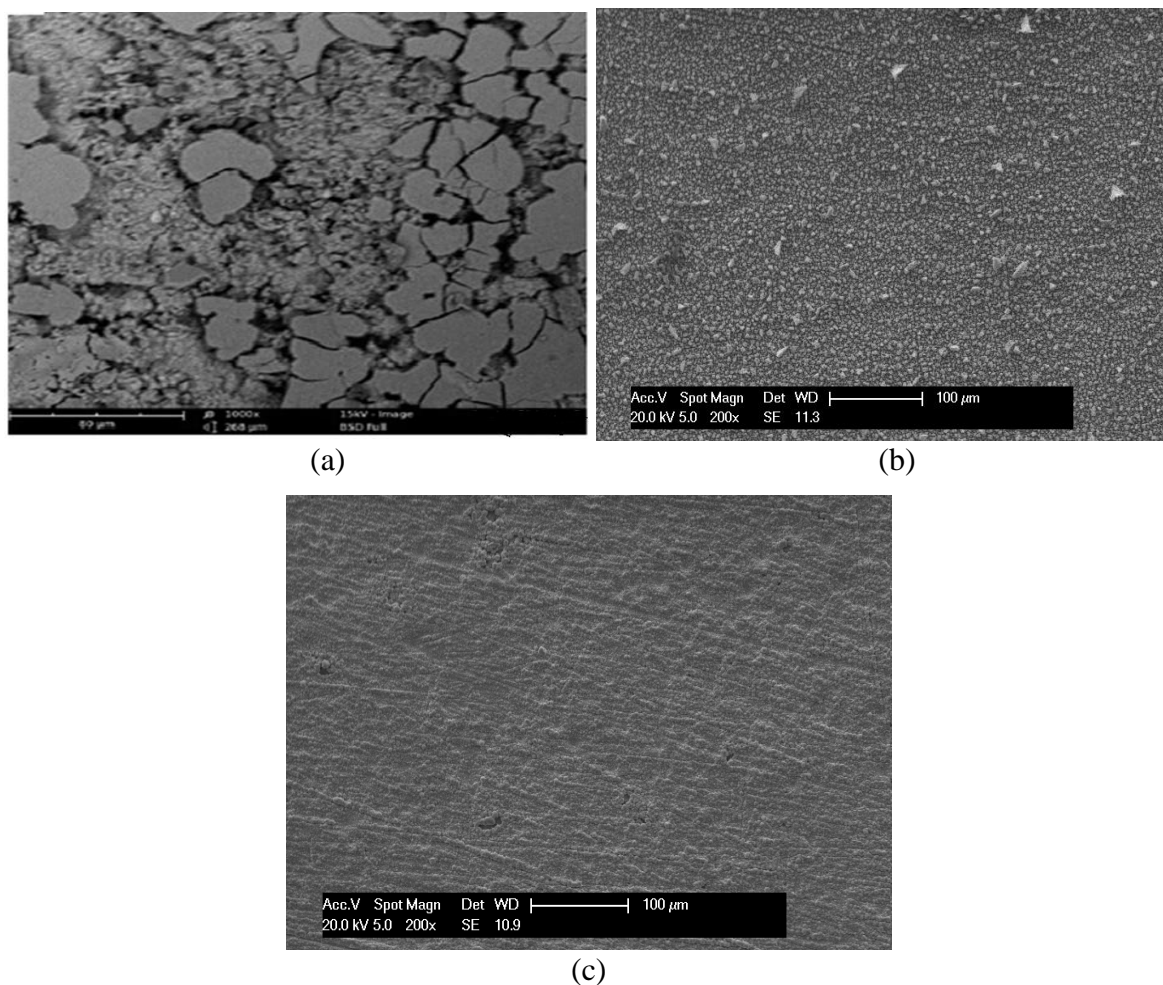


**Figure 4:** SEM diagrams for the corrosion inhibition of (a) 1 M HCl acid (b) 1.0 g/L and (c) 5.0 g/L Vindoline alkaloids on Gray Iron.

### 2.3 Thermodynamic calculations

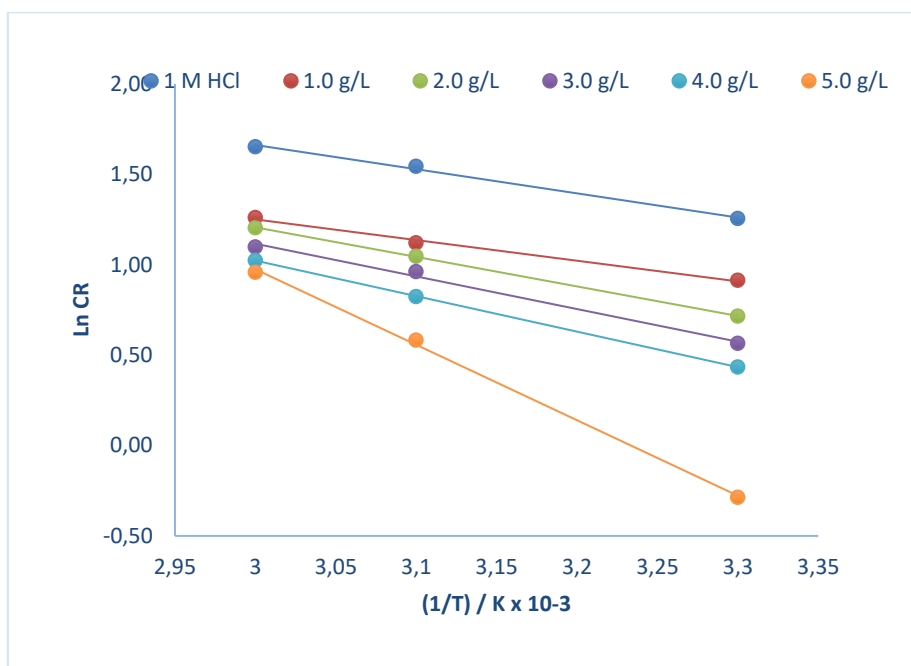
A convenient approach of determining  $E_a$  for a reaction involves the measurement of rate constant,  $k$  at different temperatures and using of an alternate version of the Arrhenius equation that takes that form of a linear equation 2 and 3.

$$k = Ae^{-\frac{E_a}{RT}} \quad \dots \quad \dots \quad \dots \quad \dots \quad 2$$

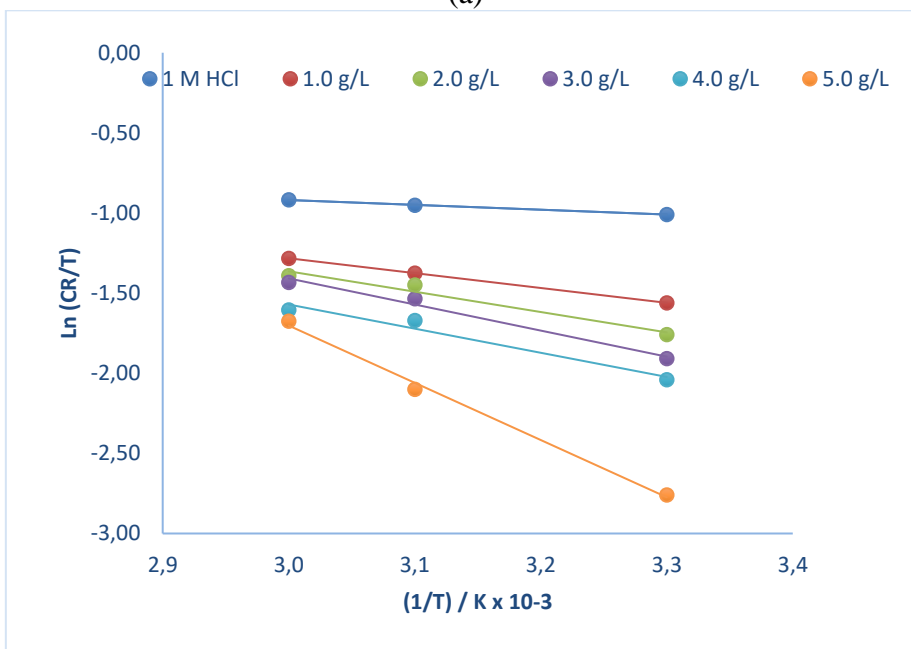
$$\ln k = \left(-\frac{E_a}{R}\right)\left(\frac{1}{T}\right) + \ln A \quad \dots \quad \dots \quad \dots \quad 3$$

Thus plot of  $\ln k$  versus  $1/T$  gives a straight line with the slope  $-\frac{E_a}{R}$ , from which  $E_a$  may be determined. The intercept gives the value of  $\ln A$  (Figure. 5a) [7, 11, 15-19], reaction that is required to activate atoms or molecules to a condition in which they can undergo chemical transformation or physical transport [13-17, 26-29]. This values also showed that as the concentration of inhibitors increases with corresponding temperature, the molecules move faster and therefore collide more frequently. The molecules also carry more kinetic energy. Thus, the proportion of collisions that can overcome the

activation energy for the inhibition reaction to occur increases with temperature, hence overcoming forces of repulsion, and start breaking bonds [22, 27-30]. It was confirmed from Table 3 that values were less than  $20 \text{ kJmol}^{-2}$  verifying a physical adsorption process and highest inhibition efficiency at lower temperatures ( ambient up to  $59^\circ \text{C}$ ) [6-10, 17, 27, 30-32]. Negative values of entropy of adsorption  $\Delta S^\ddagger$  (Figure. 5b), were recorded for the inhibitor – metal interaction, indicating that entropy decreases on forming the transition state, which often indicates an associative mechanism in which both the molecules of Vindoline alkaloids and the ions of Gray Iron surface form a single activated complex hence, creating a better inhibition process [15,19-23].



(a)

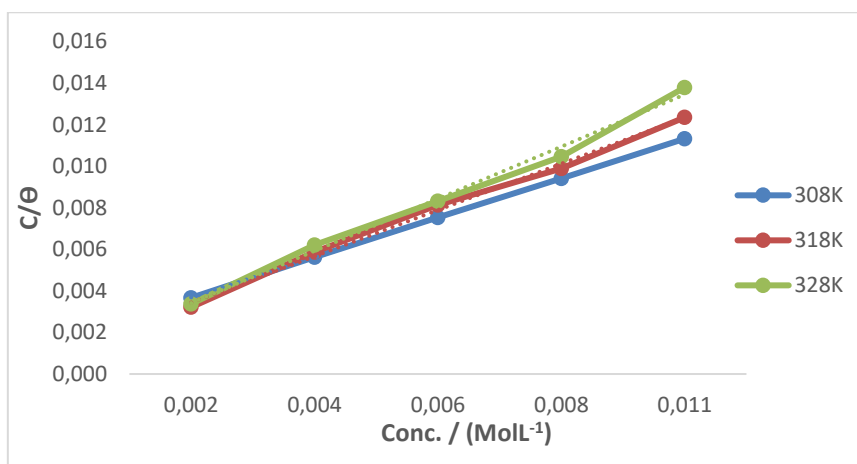


(b)

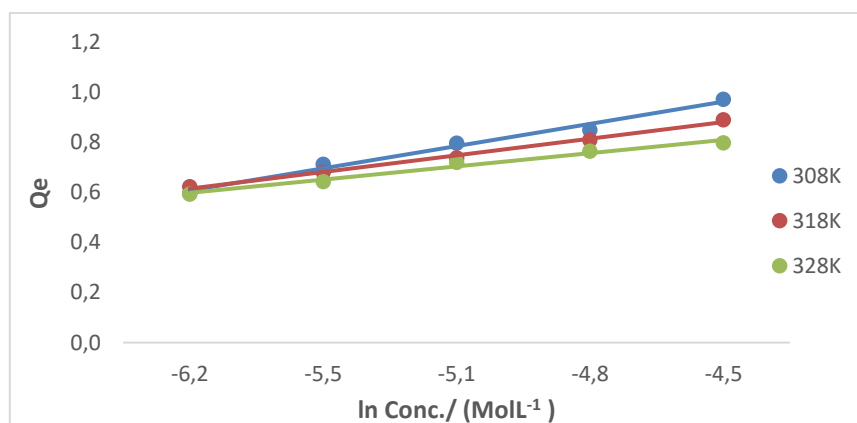
**Figure 5:** (a) Arrhenius and (b) Eyring Transition state plots for the inhibition of vindoline particles on Gray Iron in 1 M HCl solutions.



distribution of binding energies by the inhibitors at various temperatures as values were seen increasing with increase temperature [21-23, 31]. However, changes in adsorption free energy values for Temkin were less than -20 kJ/mol compared to Langmuir adsorption result signifying inhibitor's stability on the metal surface, spontaneity of the inhibitor-metal reaction and physical adsorption process [6,11, 33-36]. Comparatively, values from Langmuir isotherm being slightly more than -20 kJmol<sup>-1</sup> compared to those of Temkin explained a possible physical adsorption that may be followed by a chemical adsorption step at a later reaction process [12, 17, 29].



(a)



(b)

**Figure 6** (a) Langmuir and (b) Temkin adsorption isotherms for the inhibition of vindoline particles on Gray Iron in 1 M HCl solutions.

**Table 4:** Adsorption data for Langmuir and Temkin isotherm for the inhibition of vindoline alkaloids on Gray Iron in 1 M HCl solutions. M = 456.5 g/mol

Temp. (K)	Langmuir Isotherm				Temkin Isotherm				
	k (mol/L)	R <sup>2</sup>	Slope	$\Delta G^*_{ads}$ (kJmol <sup>-2</sup> )	K <sub>T</sub> (mol/L)	R <sup>2</sup>	Slope	$\Delta G^*_{ads}$ (kJmol <sup>-2</sup> )	b (J/mol)
308	555.5	0.9990	0.0019	- 26.5	10.55	0.9852	0.0888	- 16.3	28.8
318	833.3	0.9959	0.0022	- 28.4	10.96	0.9937	0.0665	- 16.9	39.8
328	111.1	0.9931	0.0025	- 30.1	11.25	0.9807	0.0528	- 17.6	51.7

## Conclusion

The research presented the following findings:

1. Nitrogen molecules in vindoline alkaloids from *Cetharanthus roseus* plant proved to be excellent corrosion control inhibitor for Gray Iron in 1 M Hydrochloric acid solutions at maximum experimental concentration of 5.0 g/L as inhibition efficiency from both electrochemical and gravimetric (weight loss) measurements stood at 94.2 and 99.0 % respectively.
2. Inhibitor presented a mixed type inhibition. A possibility for both reduction in anodic dissolution and cathodic hydrogen gas evolution.
3. They showed higher stability on the Gray Iron surface in 1 M Hydrochloric acid solutions, a reaction that was prompted by spontaneity in the forward direction and associative mechanism forming a single activated complex.
4. The inhibition was possible through direct adsorption on the surface of the metal, a process that was a monolayer chemisorption.
5. Inhibitor had the potential of influencing the incoming energy in the system resulting in higher potential energy and lower kinetic energy, hence breaking up the intermolecular force between the molecules, leading to a slower corrosion reaction rate.

## Funding

This research did not receive any funding from any Organization or institution. Funding was personal.

## Conflict of interest

The Authors declare that they have no conflict of interest.

## References

1. R.R. Pierre, Handbook of Corrosion Engineering. McGraw-Hill Pub. New York, 2000
2. A.O. Okewale, J.O. Olaitan, The use of rubber leaf extract as a corrosion inhibitor for mild steel in acidic solution, *Int. J. Mater. Chem.*, 2017, 7, 13 – 23.
3. N. Chandrasekaran, M. Vanitha, M. Kaavyalaskshmi, Extraction of Vindoline from *Catharanthus roseus* and instrumental model of automatic column chromatography by using PLC, *Intl. J. Chem. Tech. Res.*, 6(9) (2014) 4216 – 4224
4. K.C. Ajani, A.S. Abdulrohman, E. Mudiare, Inhibitory action of aqueous citrus curantifilia seed extract on the corrosion of mild steel in H<sub>2</sub>SO<sub>4</sub> solution, *World App. Sc. J.*, 31(12) (2014) 2141-2147.
5. C.O. Akalezi, E.E. Oguzie, Evaluation of anticorrosion properties of *Chrysophyllum Albidum* leaves extract for mild steel protection in acidic media, *Int. J. Ind. Chem.*, 7 (2016) 81-92.
6. H. Ali, H.A. Suleiman, Effects of acid extract of leaves of *Juniperus procera* on corrosion inhibition of carbon steel in HCl solution, *Int. J. Electrochem. Sci.*, 13 (2018) 3910 – 3922.
7. E. Alibakhshi, M. Ramezanzadeh, G. Bahlakeh, B. Ramezanzadeh, M. Mahdavian, M. Motamedi, Glycyrrhiza glabra leaves extract as a green corrosion inhibitor for mild steel in 1 M hydrochloric acid solution: Experimental, molecular dynamics, Monte Carlo and quantum mechanics study, *J. Mol. Liq.*, 6 (2018) 265.
8. D.A. Al-Shehri, Oil and gas wells: enhanced wellbore casing integrity management through corrosion rate prediction using an augmented intelligent approach, *Sustainability*, 11 (2019) 1-18.

9. P.O. Ameh, N.O. Eddy, Theoretical and experimental studies on the corrosion inhibition potentials of 3-Nitrobenzoic acid for mild steel in 0.1 M H<sub>2</sub>SO<sub>4</sub>, *Cogent Chemistry*, 2 (2016) 125.
10. P. R. Ammal, M. Prajila, A. Joseph, Effective inhibition of mild steel corrosion in hydrochloric acid using EBIMOT, 1,3,4-oxadiazole derivative bearing a 2- ethylbenzimidazole moiety: Electro analytical, computational and kinetic studies, *Egyptian J. Petrol.*, 27 (2018) 823-833.
11. I.C. Awe, A.S. Abdulhaman, H.K. Ibrahim, A. Kareem, A.S. Ganiyu, Inhibitive Performance of Bitter Leaf Root Extract on Mild Steel Corrosion in Sulphuric Acid Solution, *Amer. J. Mat. Engr. Tech.*, 3(2) (2015) 35-45.
12. F.A. Ayeni, I.A. Madugu, P. Sukop, A.P. Ihom, O.O. Alab, R. Okara, M. Abdulwaha, Effect of aqueous extract of bitter leaf powder on corrosion inhibition of Al-Si Alloy in 0.5 caustic Soda Solution, *J. Min. Mat. Charac. Engr.*, 11 (2012) 667-670.
13. K., Boumhara, H. Harhar, M. Tabyaoui, A. Bellaouchou, A. Guenbour, A. Zarrouk, Corrosion inhibition of mild steel in 0.5 M H<sub>2</sub>SO<sub>4</sub> solution by Artemisia herba- alba Oil, *J. Bio- and Tribo- Corros*, 5 (2019) 1-8
14. H. Cang, Z. Fei, J. Shao, W. Shi, Q. Xu, Corrosion Inhibition of Mild Steel by Aleos Extract in HCl Solution Medium, *Intl. J. Electrochem. Sc.*, 8 (2013) 720-734.
15. G. A. Cooney, B. L. Tambari, D. S. Iboroma, Evaluation of corrosion inhibition potentials of green tip forest lily (*Clivia no-bilis*) leaves extract on mild steel in acid media, *Journal of applied Sci. Env. Mgt*, 22 (1) (2018) 90 – 94
16. O. Dagdag, A. El Harfi, O. Cherkaoui, Z. Safi, L.G. Wazzan, E.D. Akpan, C. Verma, E.E. Ebenso, T.T. Jalgham, Rheological, electrochemical, surface, DFT and molecular dynamics simulation studies on the anticorrosive properties of new epoxy monomer compound for steel in 1 M HCl solution, *RSC Advances*, 9 (2019) 4454-4462.
17. B. Evgenij, R.J. Macdonald, Impedance, Spectroscopy, Theory and Experiment. 2nd ed. John Wiley and Son Pub. Canada, 2012.
18. M. A. Fajobi, O.S.I. Fayomi, I.G. Akande, O.A. Odunlami, Inhibitive Performance of Ibuprofen Drug on Mild Steel in 0.5 M of H<sub>2</sub>SO<sub>4</sub> Acid, *J. Bio- and Tribo- Corros.*, 5 (2019) 9
19. H.S. Gadow, M.M. Motawea, Investigation of the corrosion inhibition of carbon steel in hydrochloric acid solution by using ginger roots extract, *RSC Advances*, 7(40) (2017) 24576-24588.
20. T. He, W. Emori, R. Zhang, P.C. Okafor, M. Yang, C. Cheng, Detailed Characterization Of Phellodendron Chinense Schneid And Its Application In The Corrosion Inhibition Of Carbon Steel In Acidic Media, *Bio- Electrochem.*, (2019)130
21. N. Hebbar, B.M. Praveen, B.M. Prasanna, H.P. Sachin, Anticorrosion potential of flectofenine on mild steel in hydrochloric acid media: experimental and theoretical study, *J Fail Anal Prev*, 1(11) (2018) 371
22. D. Kumar, V. Jain, B. Rai, Unravelling the mechanisms of corrosion inhibition of iron by henna extract: A density functional theory study, *Corros Sci.*, 142 (2018) 102- 109.
23. S. Leelavathi, R.J. Rajalakshim, Leaves extracts as acid corrosion inhibitor for mild steel- A green approach materials, *Envir. Sc.*, 4(5) (2013) 625-638
24. H. Lgaz, R. Salghi, S. Jodeh, B. Hammouti, Effect of clozapine on inhibition of mild steel corrosion in 1.0 M HCl medium, *J. Mol. Liq.*, 225 (2017) 271–28
25. M.T. Majda, M. Ramezanzadeh, B. Ramezanzadeh, G. Bahlakeh, Production of an environmentally stable anti-corrosion film based on Esfand seed extract molecules-metal cations: Integrated experimental and computer modeling approaches, *J. Harz. Mat.*, 382 (202) 1-16.

26. A.O. Okewale , J.O. Olaitan, The use of rubber leaf extract as a corrosion inhibitor for mild steel in acidic solution, *Int. J. Mater. Chem.*, 7 (2017) 13 – 23.
27. E.F. Olasehinde, S.J. Olusegun, A.S. Adesina, H. Momoh-Yahaya, Inhibitory action of *Nicotiana tabacum* extracts on the corrosion of mild steel in HCl: Adsorption and Thermodynamics Study, *National Sc.*, 11(1) (2013) 83-90.
28. R.K. Pathak, P. Mishra, Drugs as corrosion inhibitors: A review. *Intl. J. Sc. Res.* 5(4) (2016) 671-677.
29. P. Rodic, I. Milosev , The influence of additional salts on corrosion inhibition by cerium (III) acetate in the protection of AA 7075-T6 in chloride solution, *Corros. Sci.*, 149 (2019) 108-122.
30. Srinivasulu, P.K. Kasthuri , Study of inhibition and adsorption properties of mild steel corrosion by expired pharmaceutical gentamicin drug in hydrochloric acid media. *Oriental J. Chem.*, 33(5) (2017) 2616-2624.
31. P. Su, L. Li, W. Li, C. Huang, X. Wang, Y. Liu, A. Singh, Expired drug theophylline as potential corrosion inhibitor for 7075 aluminum alloy in 1M NaOH solution, *Intl. J. Electrochem. Sc.*, 15 (2020) 1412 – 1425.
32. B.U. Ugi, M.E. Obeten, Inhibition of localized corrosion in 2205 Duplex stainless steel by expired myambutol (ethambutol hydrochloride) drug in acid catalyzed environment, *Intl. J. Innov. Sc. Res. Tech.*, 4(11) (2019b) 752 - 760
33. B.U. Ugi, M.E. Obeten, Investigating the Anticorrosion Potentials of Expired Nevirapine Antiretroviral as Inhibitor of Potential Crude Oil Steel in Acidic Medium, *Intl. Res. J. Innov. Engr. Tech*, 3(4) (2019 a) 44-50.
34. S.A. Umoren, M.M. Solomon, Effect of halide ions on the corrosion inhibition efficiency of different organic species—a re-view, *J. Ind. Eng. Chem.*, 21 (2015) 100 – 107.
35. V. Vorobyova, M. Skiba, Apricot pomace extract as a natural corrosion inhibitor of mild steel corrosion in 0.5 m NaCl solution: a combined experimental and theoretical approach, *J. Chem. Tech. Metall.*, 55(1) (2020) 210-222
36. X. Wang, H. Jiang, D. Zhang, H. Wen-jie Zhou, Solanum lasiocarpum l. extract as green corrosion inhibitor for A3 steel in 1 m HCl solution, *Int. J. Electrochem. Sc.* 14 (2019) 1178 – 1196

(2020) ; <http://www.jmaterenvironsci.com>